An efficient boundary element method for nonlinear water waves

S. T. Grilli, J. Skourup* and I. A. Svendsen

Ocean Engineering Program, Department of Civil Engineering, University of Delaware, Newark, DE 19716, USA

The paper presents a computational model for highly nonlinear 2-D water waves in which a high order Boundary Element Method is coupled with a high order explicit time stepping technique for the temporal evolution of the waves. The choice of the numerical procedures is justified from a review of the literature. Problems of the wave generation and absorption are investigated. The present method operates in the physical space and applications to four different wave problems are presented and discussed (space periodic wave propagation and breaking, solitary wave propagation, run-up and radiation, transient wave generation). Emphasis in the paper is given to describing the numerical methods used in the computation.

Key Words: Boundary Element Method, nonlinear wave analysis, solitary wave, transient wave generation, overturning wave

1. INTRODUCTION

1.1. Numerical modelling of ocean waves

The numerical modelling of ocean wave situations that aims at analyzing their nonlinear interaction with engineering structures will always require a relatively large degree of spatial resolution and, hence, can only cover a limited area in the neighborhood of the structure. Therefore such models will always contain three essential elements:

- A generation of the waves to be studied. The generation simulates the waves that in the nature just propagate into the region that has been chosen for modelling.
- An element that numerically propagates the waves through the region of computation and accounts for their interaction with structures inside the region.
- A mechanism which prevents that waves propagating outward, toward the boundary of the computational region are reflected back into the region in a non-physical manner (far field representation).

Those are essentially the same elements we find in a traditional laboratory wave tank. Therefore the numerical modelling of nonlinear ocean waves can be considered in many respects as the computational equivalent of a traditional wavetank (a 'numerical wavetank'). Several techniques have been developed for all three elements in the list, and a brief literature review is given hereafter. In most studies so far, however, starting with Longuet-Higgins and Cokelet[26] the generation and absorption of the waves (1st and 3rd elements) have been entirely avoided by assuming the waves to be two-dimensional only and to be spatially periodic in the direction of their propagation.

Paper accepted January 1989. Discussion ends February 1990.

* Present address: Institute of Hydrodynamics and Hydraulic Engineering, Technical University of Denmark, DK-2800 Lyngby, Denmark.

1.2. Solution technique

The Boundary Integral Equation Method (BIEM) and the Boundary Element Method (BEM) have been very successfully used in the solving of a large number of linear two- and a few three-dimensional wave problems. For reference one can consult the reviews by Shaw[31] and Liu and Liggett[24]. In such problems, the method offers the great advantage of describing the flow by its boundary values only (reducing the problem dimensions by one, and thus the computing time). Moreover, unlike the situation in many structural analysis problems, in the analysis of wave motions the boundary shape, and the velocity or velocity gradient on the boundary represent the only information needed in the computations. In those problems, the BEM has thus showed to be up to one order of magnitude faster, for a same accuracy, than domain discretization methods, like the Finite Element Method (Grilli[11,13]).

Applications of BIEM or BEM to nonlinear waves lead to computational models which essentially consist of two coupled parts. The first is a solution of the Laplace equation (the continuity equation in a non-viscous irrotational fluid model), at a given time. The second part is a forward stepping to the next time level at which the Laplace equation is again solved and so forth.

The time stepping consists of integrating the two nonlinear free surface boundary conditions (kinematic and dynamic) and the relevant boundary conditions along the rest of the boundary and, thereby, establishing both the new position of the boundary and the relevant boundary conditions along the new boundary at the next time step.

For the far field representation, several methods can be used, including the coupling of interior and exterior solutions.

2. BRIEF REVIEW OF THE EXISTING SOLUTIONS

2.1. The first numerical solutions

Reviews of analysis of highly nonlinear wave problems can be found in Yeung[35] and in Liggett and Liu[21]. The first contributions to the method can be divided into four parts.

1. The first successful numerical computation of 2-D steep deep water surface motions and overturning waves was made by Longuet-Higgins and Cokelet[26]. In this first publication the Laplace equation was solved by a BIEM based on 3rd Green's identity, and the idea was introduced of working in a conformally mapped space. In the time stepping they used a lagrangian description of the free surface, but approximated the partial differential expressions of the free surface boundary conditions by ordinary differential equations. The integration in time was then performed by an Adams–Bashforth–Moulton method and initiated by a Runge–Kutta scheme. This approximate time updating procedure induced sawtooth oscillations on the free surface which required smoothing procedures to be introduced. Many applications of the method can be found in the literature, up to very recently, but without any further real innovations except, perhaps, the extension to finite depth by New, McIver and Peregrine[29].
2. Vinje and Brevig[34] modified the previous method by using a Laplace solution based on Cauchy's complex integral theorem applied to the physical space, and studied finite depth breaking waves and forces on a submerged pipeline (Brevig, Greenhow and Vinje[4]). The method created less sawtooth oscillations. It was also well suited to less time-consuming iterative methods for solving the matrix equation. Their use of both velocity potential and stream function to obtain a problem formulated entirely as a Fredholm equation of the second kind was in fact already outlined by Svendsen[33].
3. The method of double layers has been utilized by Baker, Meiron and Orszag[1], who computed finite depth breaking waves and derived an efficient iterative method of solution.
4. Dold and Peregrine[7] developed an accurate explicit time stepping method by using a higher order Taylor expansion in time for the free surface position in a lagrangian formulation. To get the Taylor series coefficients, they solved a succession of Laplace problems for the velocity potential and its time derivatives, each problem solution providing the nonlinear free surface boundary condition for the next one. Their method for solving Laplace was similar to the one by Vinje and Brevig, but in a conformally mapped space. In addition to being of high order, their method of integration in time also correctly accounts for the influence of the derivatives along the surface, which were only included to lower order in Longuet-Higgins and Cokelet's time stepping method. The method allowed them to use large time steps and provided a very good stability (permitting them to avoid almost any smoothing), and it was an order of magnitude faster than Longuet-Higgins and Cokelet's method, mainly due to their large time steps.

For completeness, reference is also made to the implicit iterative time stepping methods developed by Liu and applied by Kim, Liu and Liggett[17] and Liu and Liggett[25] and the error correcting method developed by Nakayama[27].

2.2. Solutions in the physical space

As mentioned, all the contributions described above studied space periodic waves. In addition, they used complex variable relationships such as conformal mapping or the Cauchy theorem. Thus, they were also limited by nature to two dimensions.

In order to analyze waves that are not period in space, it is necessary to work in the physical space, which provides the additional advantage that we are able to extend the method to three dimensions and to introduce structures of arbitrary shape into the domain. Vinje and Brevig[34] also worked in the physical space and could introduce structures. Their method has been very successfully used and improved by Lin, Newman and Yue[23].

The combination of physical space and 3-D problems is still very rare, and poses far-field representation problems (see below). Isaacson[16] studied the 3-D nonlinear forces on structures. He used a BEM based on a 3-D free space Green's function, and a time stepping similar to that of Longuet-Higgins and Cokelet, and Dommermuth and Yue[8] studied an axisymmetric heaving problem using equivalent procedures in an axisymmetric formulation which essentially is a problem that can be described by two dimensions. Romate[36] developed a 3-D panel method he applied to weakly nonlinear waves.

2.3. Wave generation

The methods listed above can propagate the wave in space and time but, as already pointed out, it is necessary in the physical space to generate the wave motion and to absorb it.

If the waves are generated by simulating a wave maker or a body movement, singularity problems are created at the confluence of boundary conditions (Kravtchenko[18]) or numerically speaking, corner problems. To remove this singularity, Lin, Newman and Yue[23] suggested to specify both the potential and the stream function at the body part of the corner. Doing so, they could generate nonlinear waves by a wave maker. Dommermuth and Yue[8], following the same principle as Lin *et al.*, imposed both the potential and its normal derivative at the body part of the corner in their BEM formulation.

2.4. Absorption and radiation of the waves

For linear waves absorbing boundary conditions have been developed by Engquist and Majda[9]. The absorption of waves by damping was first used, for linear waves, by LeMehaute[20]. A similar idea termed a 'sponge layer' was introduced, for Boussinesq equations, by Larsen and Dancy[19]. Hybrid methods coupling the BEM solution with exterior solutions based on eigen function expansions or on flat bottom numerical solutions, have also been very successful for linear waves (Liu and Liggett[24], Grilli[11,12,13]).

For nonlinear waves of non-permanent form, however, no general absorbing or radiation condition is available. Some rather heuristic boundary conditions have been

used instead, like Isaacson[16], who simply imposed a zero velocity on the lateral boundary of the computation (corresponding to a reflecting wall), which limited the validity of the solution to a few wave periods. Other authors matched exerior linear solutions at a finte distance, like Lin, Newman and Yue[23] who coupled successfully a 3-D exterior flat bottom linear solution to a nonlinear 2-D numerical solution. Their solution was claimed to work for an indefinite time, without producing reflection, because of the energy decay in the 3-D radiated field (the corresponding 2-D solution did not work). Dommermuth and Yue[8] used the same method for the forced heaving motion of a cylinder.

2.5. *General features of our solution*

In the present paper, the Laplace equation is solved in the physical space, since we intend to generate non-periodic waves and to absorb them. The presentation is limited to problems in a 2-D model, but can in principle be extended to 3-D problems.

The solution of the Laplace problems is based on a non-complex method which is, in our case, a high order BEM, using the free space Green's function.

The time stepping is equivalent to Dold and Peregrine's which is a stable and fast method. Besides, it has the great advantages of being explicit and without the approximations of the method introduced by Longuet-Higgins and Cokelet.

The wave generation is performed by simulating a wavemaker movement in the model, or by imposing extended periodicity conditions (space periodic wave train). But other methods like the generation by internal sources (Brorsen and Larsen[5]) could equally well be implemented.

Wave absorption has so far only been implemented for constant shape waves, like the solitary or simple period waves.

Finally the very high overall stability in time of the above described method, permitted us to avoid smoothing procedures in any of the examples presented in section 5.

3. MATHEMATICAL FORMULATION

3.1. *Governing equations and boundary conditions*

We assume an inviscid irrotational flow (for the time being restricted to 2-D) described by a velocity potential $\phi(\mathbf{x}, t)$, and the velocity field is given by $\mathbf{u}=\nabla\phi=(u, w)$. Thus, the continuity equation in the fluid domain $\Omega(t)$ with the boundary $\Gamma(t)$ becomes a Laplace equation for ϕ (Fig. 1),

$$\nabla^2\phi=0 \qquad \text{in } \Omega(t) \tag{1}$$

Using the free space Green's function $G(\mathbf{x}, \mathbf{x}_l)$, this is solved as the boundary integral equation,

$$\alpha(\mathbf{x}_l)\phi(\mathbf{x}_l)=\int_\Gamma\left[\frac{\partial\phi}{\partial n}G(\mathbf{x}, \mathbf{x}_l)-\phi\frac{\partial G(\mathbf{x}, \mathbf{x}_l)}{\partial n}\right]d\Gamma \tag{2}$$

where $\mathbf{x}$ and $\mathbf{x}_l$ are the coordinates of points on the boundary, and $\alpha(\mathbf{x}_l)$ is a geometric coefficient.

On the free surface $\Gamma_f(t)$, ϕ satisfies the kinematic boundary condition,

$$\frac{D\mathbf{r}}{Dt}=\left(\frac{\partial}{\partial t}+\mathbf{u}.\nabla\right)\mathbf{r}=\mathbf{u} \qquad \text{on } \Gamma_f(t) \tag{3}$$

with $\mathbf{r}$, the position vector of a free surface fluid particle.

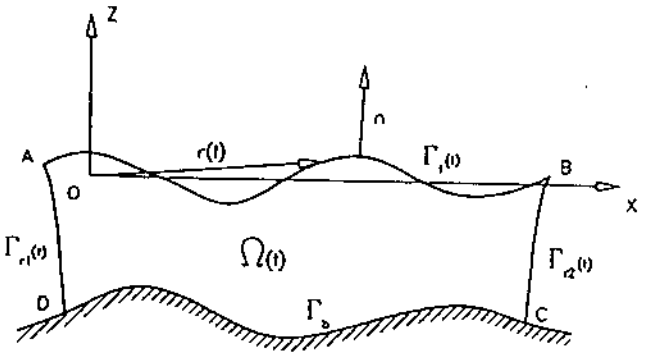

Fig. 1

Thus

$$\frac{D\mathbf{r}}{Dt}=\nabla\phi \qquad \text{on } \Gamma_f(t) \tag{4}$$

and the dynamic free surface boundary condition,

$$\frac{D\phi}{Dt}=-gz+\tfrac{1}{2}|\nabla\phi|^2-\frac{p_a}{\rho} \qquad \text{on } \Gamma_f(t) \tag{5}$$

where g is the acceleration due to gravity, z is the vertical coordinate (positive upwards and $z=0$ at the undisturbed free surface), p_a the pressure at the surface and ρ the specific mass of the fluid.

In case of wave generation by a wave maker, the normal velocity is continuous over the surface $\Gamma_{r1}(t)$ of the paddle.

$$\nabla\phi.\mathbf{n}\equiv\frac{\partial\phi}{\partial n}=V(\mathbf{x}, t) \qquad \text{on } \Gamma_{r1}(t) \tag{6}$$

where $\mathbf{n}$ is the unit outward normal vector, and V the wave maker velocity. On a stationary bottom Γ_b, (6) is satisfied with $V=0$.

In case of the absorption of a wave of permanent form with velocity c, the Sommerfeld radiation condition on the boundary $\Gamma_{r2}(t)$ reads,

$$\frac{\partial\phi}{\partial n}=-\frac{1}{c}\frac{\partial\phi}{\partial t} \qquad \text{on } \Gamma_{r2}(t) \tag{7}$$

whereas a reflection condition will be expressed by (6) with $V=0$.

In case of a space periodic wave train, $\Gamma_{r1}(t)$ and $\Gamma_{r2}(t)$ are vertical boundaries following the free surface wave particle motion. On those vertical boundaries we impose the periodicity conditions,

$$\frac{\partial\phi}{\partial n}(\Gamma_{r1}(t))=-\frac{\partial\phi}{\partial n}(\Gamma_{r2}(t)) \tag{8}$$

$$\phi(\Gamma_{r2}(t))=\phi(\Gamma_{r1}(t))+V_c(t)aL \tag{9}$$

where $V_c(t)$ is the velocity of a current uniform over the depth, L the wave train length and a is an integer number.

3.2. *The time stepping method*

The time stepping consists of integrating the two nonlinear free surface conditions (4) and (5) to establish, both the new position of the free surface and the relevant boundary conditions of Laplace's problems at the next time step. Following the approach used by Dold and Peregrine[7], the updating of $\Gamma_f(t)$ is based on a truncated Taylor expansion in a lagrangian formulation which

corresponds to following a fluid particle,

$$\mathbf{r}(t+\Delta t)=\mathbf{r}(t)+\sum_{k=1}^{n}\frac{(\Delta t)^k}{k!}\frac{D^k\mathbf{r}(t)}{Dt^k}+O[(\Delta t)^{n+1}] \tag{10}$$

$$\phi(\mathbf{r}(t+\Delta t),t+\Delta t)=\phi(\mathbf{r}(t),t)+\sum_{k=1}^{n}\frac{(\Delta t)^k}{k!}\frac{D^k(\mathbf{r}(t),t)}{Dt^k}+O[(\Delta t)^{n+1}] \tag{11}$$

To get the coefficients in the expansions, we solve a succession of Laplace problems for the velocity potential ϕ and its time derivatives, each problem solution providing the nonlinear free surface boundary conditions for the next one. Indeed, the Laplace equation (1) is valid for all the time derivatives of ϕ. In our model, the series are presently limited to the second order terms ($n=2$), but the procedure described can in principle be extended to higher order terms.

The expansion coefficients are expressed in terms of ϕ, $\partial\phi/\partial n$ and $\partial^2\phi/\partial t\,\partial n$, and of their derivatives along the free surface. We adopt a local coordinate system at the free surface defined by (s, n), the tangential and normal unit vectors to the free surface (Fig. 2). This formulation provides simpler expressions for the high order derivatives than the (x, z) system. Using,

$$\cos\beta=\frac{\partial x}{\partial s},\qquad \sin\beta=\frac{\partial z}{\partial s}$$

we obtain by (4),

$$\frac{D\mathbf{r}}{Dt}=\left[\frac{\partial\phi}{\partial s}\cos\beta-\frac{\partial\phi}{\partial n}\sin\beta,\frac{\partial\phi}{\partial n}\cos\beta+\frac{\partial\phi}{\partial s}\sin\beta\right] \tag{12}$$

The continuity and irrotationality conditions yield,

$$\frac{\partial w}{\partial z}=-\frac{\partial u}{\partial x}\quad\text{or}\quad\frac{\partial^2\phi}{\partial s^2}=-\frac{\partial^2\phi}{\partial n^2}$$

$$\frac{\partial w}{\partial x}=\frac{\partial u}{\partial z}\quad\text{or}\quad\frac{\partial^2\phi}{\partial n\,\partial s}=\frac{\partial^2\phi}{\partial s\,\partial n} \tag{13}$$

and after some calculations we get,

$$\begin{aligned}\frac{D^2\mathbf{r}}{Dt^2}=\Bigg[&\left(\frac{\partial^2\phi}{\partial t\,\partial s}+\frac{\partial\phi}{\partial s}\frac{\partial^2\phi}{\partial s^2}+\frac{\partial\phi}{\partial n}\frac{\partial^2\phi}{\partial n\,\partial s}\right)\cos\beta\\&+\left(\frac{\partial\phi}{\partial n}\frac{\partial^2\phi}{\partial s^2}-\frac{\partial\phi}{\partial s}\frac{\partial^2\phi}{\partial s^2}-\frac{\partial^2\phi}{\partial t\,\partial n}-\frac{\partial\beta}{\partial s}|\nabla\phi|^2\right)\sin\beta\\&+\left(\frac{\partial^2\phi}{\partial t\,\partial n}-\frac{\partial\phi}{\partial n}\frac{\partial^2\phi}{\partial s^2}+\frac{\partial\phi}{\partial s}\frac{\partial^2\phi}{\partial n\,\partial s}+\frac{\partial\beta}{\partial s}|\nabla\phi|^2\right)\cos\beta\\&+\left(\frac{\partial^2\phi}{\partial t\,\partial s}+\frac{\partial\phi}{\partial s}\frac{\partial^2\phi}{\partial s^2}+\frac{\partial\phi}{\partial n}\frac{\partial^2\phi}{\partial n\,\partial s}\right)\sin\beta\Bigg]\end{aligned} \tag{14}$$

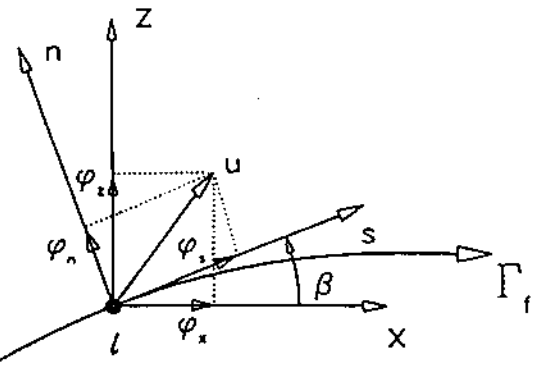

Fig. 2

In the same way, $D\phi/Dt$ is obtained from (5) and we then get,

$$\begin{aligned}\frac{D^2\phi}{Dt^2}=&\frac{\partial\phi}{\partial s}\frac{\partial^2\phi}{\partial t\,\partial s}+\frac{\partial\phi}{\partial n}\frac{\partial^2\phi}{\partial t\,\partial n}+\frac{\partial\phi}{\partial s}\left(\frac{\partial\phi}{\partial s}\frac{\partial^2\phi}{\partial s^2}+\frac{\partial\phi}{\partial n}\frac{\partial^2\phi}{\partial n\,\partial s}\right)\\&-\frac{\partial\phi}{\partial n}\left(\frac{\partial\phi}{\partial n}\frac{\partial^2\phi}{\partial s^2}-\frac{\partial\phi}{\partial s}\frac{\partial^2\phi}{\partial n\,\partial s}\right)+\frac{\partial\phi}{\partial n}|\nabla\phi|^2\frac{\partial\beta}{\partial s}\\&-g\left(\frac{\partial\phi}{\partial n}\cos\beta+\frac{\partial\phi}{\partial s}\sin\beta\right)-\frac{1}{\rho}\frac{Dp_a}{Dt}\end{aligned} \tag{15}$$

where Dp_a/Dt is the total rate of change of the surface pressure in time. After solving the Laplace problem at time t, for ϕ and $\partial\phi/\partial n$, we express the boundary conditions for the $\partial\phi/\partial t$ and $\partial^2\phi/\partial t\,\partial n$ problem. By (5)–(9) and (13) we get,

$$\frac{\partial\phi}{\partial t}=-gz-\tfrac{1}{2}|\nabla\phi|^2-\frac{p_a}{\rho}\qquad\text{on }\Gamma_f(t) \tag{16}$$

$$\frac{\partial^2\phi}{\partial t\,\partial n}=0\qquad\text{on }\Gamma_b \tag{17}$$

For the wave generation,

$$\frac{\partial^2\phi}{\partial t\,\partial n}=\frac{\partial V(\mathbf{x},t)}{\partial t}\qquad\text{on }\Gamma_{r1}(t) \tag{18}$$

and using (1),

$$\frac{\partial^2\phi}{\partial t\,\partial n}=c\frac{\partial^2\phi}{\partial s^2}\qquad\text{on }\Gamma_{r2}(t) \tag{19}$$

For the space periodic wave train,

$$\frac{\partial^2\phi}{\partial t\,\partial n}(\Gamma_{r1}(t))=-\frac{\partial^2\phi}{\partial t\,\partial n}(\Gamma_{r2}(t)) \tag{20}$$

$$\frac{\partial\phi}{\partial t}(\Gamma_{r2}(t))=\frac{\partial\phi}{\partial t}(\Gamma_{r1}(t))+\frac{\partial V_c(t)}{\partial t}aL \tag{21}$$

4. NUMERICAL IMPLEMENTATION

4.1. Solution of Laplace's equation by a high order BEM

4.1.1. Principle of solution

Provided we know the initial conditions at given time, i.e. the domain $\Omega(t)$ and the solutions to the above mentioned Laplace problems, we can update the free surface position and the free surface potential to the next time step. A first Laplace problem is defined for ϕ and $\partial\phi/\partial n$ by (1) and (5)–(9). Its solution provides the boundary conditions of a second Laplace problem for $\partial\phi/\partial t$ and $\partial^2\phi/\partial t\,\partial n$. Both Laplace problems are expressed in the same geometry $\Omega(t)$ which makes their numerical solution very fast. In case of the absorption condition (7) the first Laplace problem can not be solved directly, because of the unknown value of $\partial\phi/\partial t$ on Γ_{r2} at the new time step. An iterative predictor–corrector method described in 4.3 is implemented for that purpose. Since each iteration is performed in the same domain geometry, it again makes the method very efficient.

4.1.2. Boundary Integral Equations (BIE)

We solve the Laplace problems for ϕ and $\partial\phi/\partial t$, by a Boundary Element Method (BEM), based on (2). A set of N_Γ collocation nodes is used to describe the variation along the boundary (Brebbia[3], Banerjee and Butter-

field[2]). Thus we write

$$\alpha(\mathbf{x}_l)u(\mathbf{x}_l)=\int_\Gamma\left[\frac{\overline{\partial u}}{\partial n}G-u\frac{\partial G}{\partial n}\right]d\Gamma+\int_\Gamma\left[\frac{\partial u}{\partial n}G-\bar{u}\frac{\partial G}{\partial n}\right]d\Gamma$$
$$l=1,\ldots,N_\Gamma \tag{22}$$

with u as the unknown field (either ϕ or $\partial\phi/\partial t$) and $\bar{u}$, $\overline{\partial u/\partial n}$ some values prescribed by the boundary conditions. $G\equiv G(\mathbf{x},\mathbf{x}_l)$ is the Laplace problem Green's function given in two dimensions by,

$$G=-\frac{1}{2\pi}\log r$$
$$\frac{\partial G}{\partial n}=-\frac{1}{2\pi}\frac{\mathbf{r}.\mathbf{n}}{r^2}$$
$$r=|\mathbf{r}|,\qquad \mathbf{r}=\mathbf{x}-\mathbf{x}_l \tag{23}$$

r is the distance from the integration point $\mathbf{x}$ to the collocation point $\mathbf{x}_l$, belonging to the boundary Γ. Γ_n is all parts of the boundary where $\overline{\partial u/\partial n}$ is imposed (Neuman condition), and Γ_d all parts where $\bar{u}$ is imposed (Dirichlet condition). Depending on the case we get (Fig. 1):

For a wave generation problem,

$$\Gamma_n\equiv\Gamma_{r1}\cup\Gamma_{r2}\cup\Gamma_b\qquad\Gamma_d\equiv\Gamma_f \tag{24}$$

For a space periodic wave train problem,

$$\Gamma_n\equiv\Gamma_{r1}\cup\Gamma_b\qquad\Gamma_d\equiv\Gamma_f\cup\Gamma_{r2} \tag{25}$$

The $\alpha(\mathbf{x}_l)$ coefficients are functions of the interior angle θ of the boundary at x_l,

$$\alpha(\mathbf{x}_l)=\frac{\theta}{2\pi} \tag{26}$$

4.1.3. Discretization

To perform the integrations involved in exact equations of the type (22) the boundary is divided into elements. Within the k-th element Γ_e^k both the boundary geometry and the field functions (u, $\partial u/\partial n$) are discretized using the same high order shape functions (isoparametric elements). The number of elements is M and there are m nodes per element. These shape functions are analytically defined on a simple reference element Γ_ξ, to which the M 'physical' elements, of complex shape, are related by a change of variable (Fig. 3).

The use of high order shape functions increases the rate at which an approximate solution converges to the exact solution, when reducing the normalized size h of the discretization, i.e. the average distance between two boundary nodes. This rate is indeed proportional to h^m for an m-node element (Nam Seo[28]).

The cubic splines, used by some authors (see e.g. Liggett and Salmon[22]), provide a good accuracy because they ensure the inter-element continuity of the slope. However, they have been demonstrated to be time consuming (Nam Seo[28]), and they require the specification of the slope at the extremities of the free surface, which is unknown in case of wave generation in the physical space.

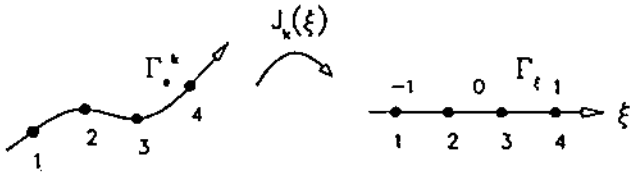

Fig. 3

The intrinsic coordinate on the isoparametric reference element Γ_ξ is ξ and $\xi\in[-1,1]$. The variation of the fields $\mathbf{x}$, u, $\partial u/\partial n$ over each element of Γ is described by their nodal values $\mathbf{x}_j$, U_j, $\partial U_j/\partial n$ respectively, where j numbers the nodes within each element, and by the shape functions $N_j(\xi)$ as,

$$\mathbf{x}=N_j(\xi)\mathbf{x}_j$$
$$u(\xi)=N_j(\xi)U_j,\qquad\frac{\partial u(\xi)}{\partial n}=N_j(\xi)\frac{\partial U_j}{\partial n}$$
$$j=1,\ldots,m;\qquad\text{on }\Gamma_\xi \tag{27}$$

Notice that the summation convention is used for repeated subscripts. To determine the coefficients in the shape functions, we require that $u(\xi)$ in (27) takes the value U_i at the nodal point $\mathbf{x}_i$, that is,

$$u(\xi(\mathbf{x}_i))=N_j(\xi_i)U_j=U_i$$

We get for the i-th node of an m-node reference element,

$$\xi_i=(2i-m-1)/(m-1)$$
$$N_j(\xi_i)=\delta_{ij}\qquad i,j=1,\ldots,m;\qquad\text{on }\Gamma_\xi \tag{28}$$

where δ_{ij} is the Kronecker's symbol.

$N_j(\xi)$ is assumed to be a polynomial which hence is of degree $m-1$ in ξ. Therefore (28) gives the corresponding polynomial coefficients. For example, in case of a cubic reference element ($m=4$) we get,

$$N_1(\xi)=\tfrac{1}{16}(1-\xi)(9\xi^2-1)$$
$$N_2(\xi)=\tfrac{9}{16}(1-\xi^2)(1-3\xi)$$
$$N_3(\xi)=\tfrac{9}{16}(1-\xi^2)(1+3\xi)$$
$$N_4(\xi)=\tfrac{1}{16}(1+\xi)(9\xi^2-1) \tag{29}$$

4.1.4. Transformation of coordinates, high order s-derivatives

The change of variables from the k-th physical boundary element of Γ: Γ_e^k to the reference element Γ_ξ (Fig. 3), is described by the Jacobian of the transformation, which by (27) is,

$$J_k(\xi)=\frac{\partial s(\xi)}{\partial\xi}=\left[\left(\frac{dN_j(\xi)}{d\xi}x_j\right)^2+\left(\frac{dN_j(\xi)}{d\xi}z_j\right)^2\right]^{\frac{1}{2}}$$
$$j=1,\ldots,m;\qquad k=1,\ldots,M\qquad\text{on }\Gamma_\xi \tag{30}$$

In the same way, the outward normal vector is given by (Fig. 2),

$$\mathbf{n}(\xi)=(-\sin\beta,\cos\beta)=\frac{1}{J_k(\xi)}\left[-\frac{dN_j(\xi)}{d\xi}z_j,\frac{dN_j(\xi)}{d\xi}x_j\right] \tag{31}$$

Using v to denote either of the variables ϕ, $\partial\phi/\partial n$ or $\partial\phi/\partial t$ and V_j to represent their nodal values, we have,

$$\frac{\partial v}{\partial s}=\frac{1}{J_k(\xi)}\frac{dN_j(\xi)}{d\xi}V_j$$
$$\frac{\partial^2 v}{\partial s^2}=\frac{1}{J_k(\xi)}\left[\frac{d^2N_j(\xi)}{d\xi^2}-\frac{1}{J_k(\xi)}\frac{dN_j(\xi)}{d\xi}\frac{d^2N_i(\xi)}{d\xi^2}(\cos\beta x_i+\sin\beta z_i)\right]V_j$$

$$\frac{\partial \beta}{\partial s}=\frac{1}{(J_k(\xi))^2}\frac{d^2N_i(\xi)}{d\xi^2}(\cos\beta z_i-\sin\beta x_i) \tag{32}$$

from which the various s-derivatives in (14) and (15) can be determined.

The description (27) of the fields inside each element, only provides a continuity between the elements of the fields themselves, not their derivatives. For the evaluation of the s-derivatives (32), we use a sliding 4th order element, independent of the above described discretization. It provides a local continuity on the boundary Γ_f of at least the 2nd s-derivatives computed at a node l identified as its central node. After each computation, the whole element is moved forward to the node $l+1$. However, it will have to remain in the same place for both the three first and the three last nodes of Γ_f (except when a space periodic problem is considered).

4.1.5. Discretization of the BIE

The equation (22), discretized by (27) and (30), leads to a linear algebraic system of equations. For consistency the boundary conditions $\overline{u_s}$ and $\overline{\partial u_p/\partial n}$ have been discretized in the same way as u and $\partial u/\partial n$. Here s refers to nodes on boundary section Γ_d (total N_{Γ_d} nodes) and p refers to nodes on Γ_n (total N_{Γ_n} nodes). We get,

$$[c_{pl}+K_{n_pl}]U_p-K_{d_{sl}}\frac{\partial U_s}{\partial n}=K_{d_{sl}}\overline{\frac{\partial U_p}{\partial n}}-[c_{sl}+K_{n_{sl}}]\overline{U_s} \tag{33}$$

with the following definitions (using j for s or p),

$$K_{n_{pl}}=\sum_{k=1}^{M}\int_{\Gamma_k}N_j(\xi)\frac{\partial G(\mathbf{x}(\xi),\mathbf{x}_l)}{\partial n}J_k(\xi)d\xi=\sum_{k=1}^{M}I^k_{n_{pl}}$$

$$K_{d_{sl}}=\sum_{k=1}^{M}\int_{\Gamma_k}N_j(\xi)G(\mathbf{x}(\xi),\mathbf{x}_l)J_k(\xi)d\xi=\sum_{k=1}^{M}I^k_{d_{sl}}$$

$$j,l=1,\ldots,N_\Gamma;\qquad s=1,\ldots,N_{\Gamma_d}$$

$$p=1,\ldots,N_{\Gamma_n};\qquad N_\Gamma=N_{\Gamma_d}+N_{\Gamma_n} \tag{34}$$

$K_{n_{pl}}$ represents integrals with $\partial G/\partial n$ and $K_{d_{sl}}$ integrals with G.

The term c_{jl} represents a diagonal matrix. Its diagonal c_{ll} is equivalent to the geometric coefficients $\alpha(\mathbf{x}_l)$. Instead of computing the c_{ll} by a direct numerical evaluation of the angles θ in (26), these coefficients are deduced by considering a particular Dirichlet problem where a uniform field $\bar{u}$ is applied on the whole boundary $\Gamma\equiv\Gamma_d$ (Brebbia[3]). In such a case, the normal gradients $\partial u/\partial n$ must vanish at each node. Thus by (33),

$$[c_{jl}+K_{n_{jl}}]\bar{U}_j=0,\qquad \bar{U}_j=c_{ss}\neq 0 \tag{35}$$

or by isolating the diagonal terms of (35),

$$[c_{ll}+K_{n_{ll}}]=-\sum_{j(\neq l)}K_{n_{jl}}\qquad j,l=1,\ldots,N_\Gamma \tag{6}$$

which provides the diagonal term of a row of (35) by minus the sum of its off-diagonal coefficients. This method can be shown to be of the same nature as the method suggested by Hsiao and McCamy[15], in which the conditioning of systems such as (33) was improved by introducing a correction term σ into a Dirichlet problem imposing the exact fulfilment of a zero-global-flux condition. The comparison of numerical results in which the c_{ll} were directly computed or deduced from (36) showed, in our case, a decrease of the system matrix condition number of more than one order of magnitude.

Finally it should be pointed out, that in (33) the only approximation is the use of shape functions to interpolate inside the M elements.

4.1.6. Computation of matrix terms

Due to the high order shape functions, the integrals involved in (34) can not be calculated analytically on each element. When the collocation node l doesn't belong to the integrated element, a standard Gauss–Legendre quadrature is used. When it does belong to the element r becomes zero at one of the nodes and special techniques are used for computing both $I^k_{d_{sl}}$ and $I^k_{n_{sl}}$ (Grilli[11]; Bruch, Grilli and Lejeune[6]; Grilli[13]).

In the intervals where $r=0$, we extract the singularity by adding and subtracting $\log|\xi-\xi_l|$. For each of the integrals,

$$I^k_{d_{sl}}=\int_{\Gamma_k}G(\xi)f^k_j(\xi)d\xi,\qquad f^k_j(\xi)=N_j(\xi)J_k(\xi)$$

in (34), we get after some transformations,

$$\begin{aligned}I^k_{d_{sl}}=-\frac{1}{2\pi}\int_{-1}^{+1}\Bigg[&\log\frac{2r_l(\xi')}{|\xi'-\xi_l|}f^k_j(\xi')\\&+\xi_{p1}\log\xi_{p1}f^k_j(\xi_{p1}\xi'-\xi_{p2})\\&+\xi_{p2}\log\xi_{p2}f^k_j(\xi_{p2}\xi'+\xi_{p1})\Bigg]d\xi'\\+\frac{1}{\pi}\int_0^1&[\xi_{p1}f^k_j(\xi_l-2\xi_{p1}\xi')\\&+\xi_{p2}f^k_j(\xi_l+2\xi_{p2}\xi')]\log\frac{1}{\xi'}d\xi'\end{aligned} \tag{37}$$

with ξ_l given by (28), in the case of a m-node element, and $\xi_{p1}=(\xi_l+1)/2$, $\xi_{p2}=(\xi_l-1)/2$. In (37) one can easily show, that the first integral is not singular. Thus a Gauss–Legendre quadrature formula is used. The second is weakly singular and can be integrated by the Berthod–Zaborowsky quadrature formula (Stroud and Secrest[32]), which provides the same error properties for the singular logarithmic kernel as the Gauss–Legendre formula does for non-singular integrals.

The accuracy of the computation of $I^k_{n_{sl}}$ also needs to be improved when $r\simeq 0$, although this integral is not singular. This integration is based on a change of variable, similar to the one performed by Longuet-Higgins and Cokelet[26],

$$\mu_l(\xi)=\arctan\frac{z(\xi)-z_l}{x(\xi)-x_l} \tag{38}$$

coupled to an analytic integration by parts, which makes it possible to avoid any numerical s-derivation. We have, for an m-node element (Fig. 2), that,

$$I^k_{n_{sl}}=\int_{\Gamma_k}\frac{\partial G(\xi)}{\partial n}N_j(\xi)J_k(\xi)d\xi$$

becomes,

$$I^k_{n_{sl}}=\frac{1}{2\pi}\left[\mu_l(-1)\delta_{1j}-\mu_l(1)\delta_{mj}+\int_{-1}^{1}\frac{dN_j(\xi)}{d\xi}\mu_l(\xi)d\xi\right] \tag{39}$$

Since μ_l can be singular when $x(\xi)=x_l$, the formulae (38) and (39) are only valid for elements in which the 'element slope' (slope of a straight line from node 1 to node m) is

$|\mu_1(1)| \leqslant 45°$. If this is not the case, x and z must simply be permuted in the definition (38) of μ_1, and the right hand side of (39) multiplied by -1. The integral in (39) is regular and again performed by the Gauss–Legendre quadrature formula. Terms such as (39) are zero for straight line elements, and very small for gently curved ones. However, due to the high curvature in the crest of a wave approaching breaking, those terms can become very important and require a lot of care.

In each element, we use N_{ip} integration points, and N_{ip} is chosen to be even in order to avoid having integration points at $\xi = 0$. In the examples shown in section 5, up to 8 integration points have been used (for the case of $m = 4$). In regions of Γ_f with high curvature and concentration of nodes, however, we have used 12 integration points mainly because of the rapid variation of the jacobian within the elements. This problem could also be solved by redistributing the nodes ('regriding', Dommermuth and Yue[8]). Properly done using the interpolation functions already in the computation this would not represent an actual smoothing.

4.2. Behavior near the corners

In the domain corners A through D (Fig. 1) we use double nodes to describe the integrand of (22). The coordinates of the two nodes are the same but their normal vectors differ and reflect that they belong to the two different parts of the boundary. Also $\partial\phi/\partial n$ is different at the two nodes of a corner. In the two representations of (22) thus created at points with the same position, continuity of ϕ is imposed.

At C and D this simply replaces one of the representations of (22). At the free surface corners A and B, the procedure depends slightly on which problem is considered. In the study of periodic waves, periodicity conditions are used to control the unknowns (in addition to continuity in ϕ). In the case of wave generation the local boundary conditions are used to replace one of the representations of (22). For reasons of space limitations the details are left our here.

The introduction of these 'compatibility' conditions at the double-nodes reduces the condition number of the system matrix significantly, and the accuracy of the solution is thereby dramatically improved close to the corner nodes. The integration of the rapidly varying ϕ in the corner region (shown to be theoretically logarithmic by Kravtchenko[18]) in case of the wave generation is automatically accounted for in our model by the Berthod–Zaborowsky integration technique mentioned above.

4.3. Absorption of a constant shape wave

The wave absorption on Γ_{r2}, in the case of constant shape waves, is performed by using the implicit boundary conditions (7) and (19). The following iterative method is implemented for that purpose. After updating the domain to the new geometry $\Omega(t + \Delta t)$, the two Laplace problems for ϕ and $\partial\phi/\partial t$ are solved at time $t + \Delta t$, starting from a first prediction of $\partial\phi/\partial t$ given by its value at time t. After predicting $\partial\phi/\partial t$ on Γ_{r2}, the Laplace problem for ϕ is solved by using (7), and then the one for $\partial\phi/\partial t$ by using (19). Hence a corrected value of $\partial\phi/\partial t$ is computed on Γ_{r2}, equal to the mean of its previously and newly computed values. The process is repeated until an iteration criterion is reached.

It must again be pointed out, that the domain geometry remains the same during all the iterations. Thus the latter only constitute new 'loading' vectors of (33), which are solved very fast.

4.4. Updating of the lateral boundaries

For a solution in the physical space, the lateral boundaries Γ_{r1} and Γ_{r2} (Fig. 1) must be updated after each time step. In the periodic wave train problem, these boundaries remain vertical and follow the movements of the corner nodes A and B. However, small numerical errors occur after each step. Their effect of invalidating the periodicity of the wave train is removed by using the mean value of the movements in A and B and similarly for ϕ and its derivatives with respect to t, s and n. In case of the wave generation, Γ_{r1} follows exactly the wave maker movement, while Γ_{r2} is fixed in case of a reflection boundary, or moves with the particles, in case of a constant shape wave radiation.

4.5. Checks of accuracy

The global accuracy of the numerical scheme depends on the two numerical processes we isolated before, i.e., the solution of the Laplace problems at a given time, which requires the use of a spatial discretization, and the time integration which requires a temporal one. Each of these processes can be separately checked.

A global check of the accuracy of the Laplace solution is provided by the continuity error ε_c relative to the initial volume V^i of the domain Ω,

$$\varepsilon_c = \left[\int_\Gamma \frac{\partial\phi}{\partial n}\, d\Gamma\right] \Delta t / V^i \tag{40}$$

and by the condition number k_2 of the algebraic system (33), which is an indicator of the well-posedness of the problem boundary conditions. We have,

$$k_2 = \left[\frac{\lambda^{\max}(K_{jl}K_{lj})}{\lambda^{\min}(K_{jl}K_{lj})}\right]^{\frac{1}{2}} \tag{41}$$

with K_{jl}, the system matrix of (33), and $\lambda^{\max}$, $\lambda^{\min}$, maximum and minimum eigenvalues respectively.

A global check of the time stepping accuracy is provided by the volume error ε_v relative to V^i, and by its comparison with ε_c. We have,

$$\varepsilon_v = \left[\int_\Gamma z dx - V^i\right] \Big/ V^i \tag{42}$$

One of the most demanding tests for the entire program, however, is to let it propagate a steep nonlinear wave of constant form determined, e.g. from a high order stream function approximation (Rienecker and Fenton[30]). Results of such a computation can easily be checked by calculating some characteristics of the wave whose exact value are known such as:

the mean water level $\bar{z}$,

$$\bar{z} = \frac{1}{aL}\int_{\Gamma_f} z dx \tag{43}$$

and the total energy E_T, computed as the sum of the kinetic energy E_K and potential energy E_P, where,

$$E_K = \frac{\rho}{2aL}\int_\Gamma \phi \frac{\partial\phi}{\partial n}\, d\Gamma$$

$$E_P = \frac{\rho g}{2aL}\int_{\Gamma_f} z^2 dx$$

$$E_T = E_K + E_P \qquad (44)$$

The integrals of (43) and (44) can easily be computed by introducing the discretization (27) and (30).

5. APPLICATIONS

The model has been applied to the four different situations listed below, for which some preliminary results have already been published (Grilli, Skourup and Svendsen[14]).

1. The propagation of a periodic wave of permanent form where we utilize the periodicity to close the physical space (creating situations equivalent to those studied by Dold and Peregrine[7]).
2. The propagation of a very steep sine wave which rapidly develops into a plunging breaker (corresponding to the situations examined by Longuet-Higgins and Cokelet[26]).
3. The generation of a solitary wave generated by a piston type wave maker and its run-up on a slope (as studied by several authors including Kim, Liu and Liggett[17]).
4. A transient wave generated by an articulated wave maker (Lin, Newman and Yue[23]).

The results from the computations are briefly described below. The purpose is to demonstrate the versatility, and the accuracy of the approach. It is worthwhile to emphasize that no smoothing procedures have been used.

5.1. Space periodic waves propagating in physical space

An initially periodic nonlinear wave is generated by using the Rienecker and Fenton[30] method for waves of permanent form (with 24 Fourier components). The physical dimensions are a depth $d = 10$ m, a wave height $H = 1$ m, a wave period $T = 6.14$ s and a wave length $L = 50.2$ m. This type of situation for which conformal mapping is normally used with the BIEM and which has been used in the past to study the overturning of waves. The wave conditions tested were introduced at time $t = 0$. A region of one wave length was analyzed, and the program let the wave propagate in time. The boundary was discretized into 30 cubic elements ($m = 4$), with a total of 92 nodes of which 49 were placed on the free surface. The C.P.U. time was 0.38 s (IBM 3090) per computed time step.

Fig. 4 shows the computed free surface at different times of one wave period. Time steps of $\Delta t = T/20 \approx 0.31$ s were used for the results in this figure.

The continuity error $|\varepsilon_c|$ and the error of E_T were less than 2.10^{-5}% and 2.10^{-4}% respectively, in the Laplace solution. The condition number k_2 varied between 245 and 283 during one period, or 2.7 to 3.1 times N_Γ, which is excellent. An error in total energy of 0.1% per time step develops during the time stepping. This error can be decreased by a reduction of the time step size. A time step of $T/30$ reduces the error to approximately 8/27, and a time step of $T/60$ reduces it further to 1/8 of that, This is consistent with the third order accuracy of the time integration.

The fluctuations of the mean water level $\bar{z}$ over one wave period are less than 0.005% of the wave height, even for $\Delta t = T/20$, indicating the high degree of accuracy with which the program operates.

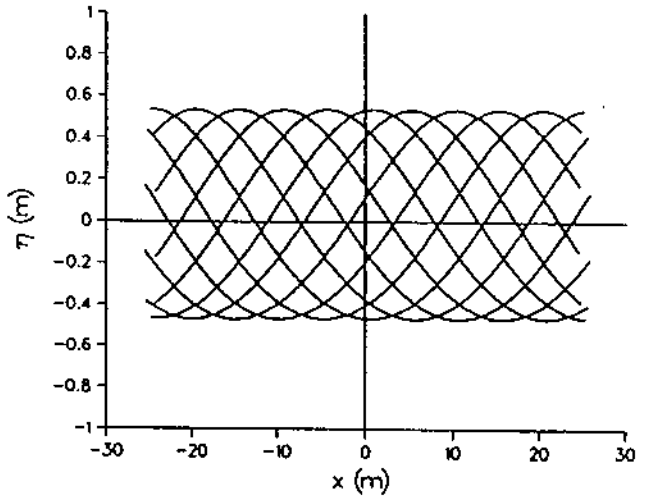

Fig. 4. Periodic wave (d = *10 m*, T = *6.14 s*, dt = T/*20*). *Stream fct. wave* (H/L = *0.02*), T/*10 to* T, *each* T/*10*

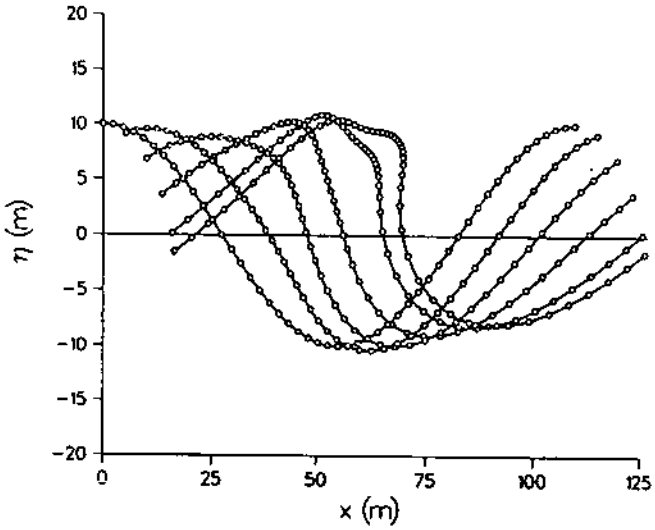

Fig. 5. Overturning wave (d = *60 m*, T = *8.40 s*, dt = T/*120*). *Instability of sinusoidal wave, 0.0 to 3.15 s, each 0.63s*

5.2. The breaking of a sinusoidal wave

Numerical experiments with the periodical version of the model also included the development of a wave with form and boundary conditions corresponding to a linear sinusoidal wave. Longuet-Higgins and Cokelet[26] found that such a wave breaks very rapidly.

The physical dimensions were $d = 60$ m, $H = 20$ m, $T = 8.40$ s and $L = 110$ m. The discretization of the boundary was the same as in the previous example, and thus the C.P.U. time per step.

Fig. 5 shows the results of the numerical experiment up to the last instant before the overturning of the wave. Time steps of $\Delta t = T/120 = 0.07$ s were used for the results in this figure. The computations were continued further with smaller Δt, and the initial stages of a plunging breaker obtained (Fig. 6).

In this application, k_2 increased from approximately 3.3 times N_Γ, in the beginning of the computation, to 4 times that value when the wave started overturning, which is still satisfactory since all the computations are performed in double precision.

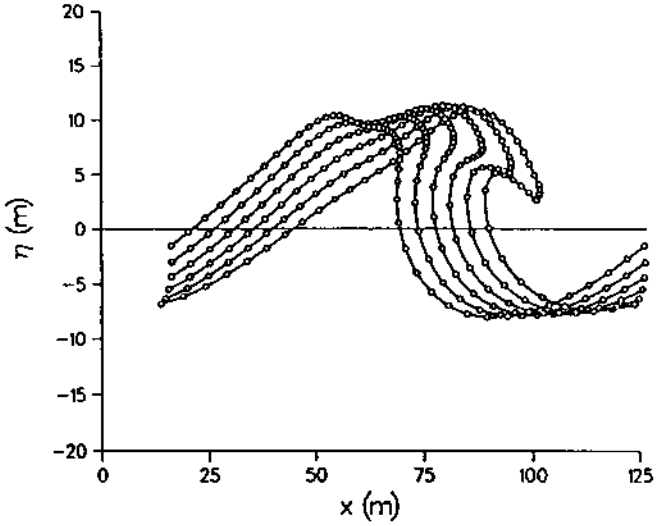

Fig. 6. Overturning wave (d = *60 m*, T = *8.40 s*, dt = T/*500*). *Curves every 0.336 s, from 3.15 s*

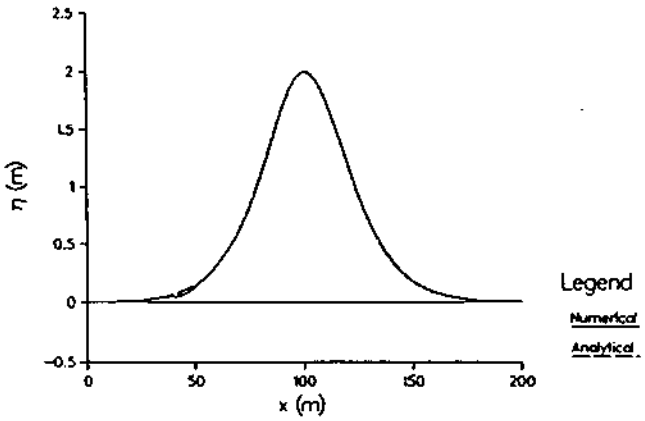

Fig. 7. Solitary wave (H/d = *0.2*, d = *10 m*, dt = *0.2 s*). *Time: 18.4 s*

5.3. A solitary wave propagation study

Solitary waves have been studied by many authors using various methods. Their reflection on vertical walls or run-up on slopes have also been investigated and used for comparisons. In the present study, a steep solitary wave is generated by using a vertical piston type wave maker, whose movement is determined from a first order solitary wave theory (Goring[10]). The physical dimensions were $d = 10$ m for a computational region 200 m long. The boundary was discretized into 38 quadratic elements ($m = 3$), with a total of 80 nodes of which 41 were placed on the free surface. Time steps of 0.2 s were used. The C.P.U. time was 0.58 s (IBM 3090) per computed time step. In that time, 61% corresponded to the computation of the BEM matrix (34), 12% to the solving of (33) for the two Laplace problems, 2% to the time updating of the domain to the next step, and 25% to postprocessing, printing and saving for plotting purpose.

For a solitary wave predicted by the first order theory to be 0.2 times the water depth, Fig. 7 shows a comparison of the generated wave with the analytical profile after propagation over 10 water depths ($t = 18.4$ s). The agreement between them is excellent (the generated solitary wave is 0.2005 times the depth). In Fig. 8, the wave is reflected on a vertical wall modelled at $x = 200$ m. Two other run-up problems have been studied. Fig. 9 shows for the last 100 m of the computation domain, stages of the run-down of the solitary wave, after its run-up on a 45 degree slope (the wave moves from up to down in this figure), and Fig. 10 shows the last 30 m of the run-up on a 15 degree slope.

In those problems the errors $|\varepsilon_c|$ and $|\varepsilon_u|$ go up to 9.10^{-6}% and 0.01%, respectively, over the first 12 seconds. After that, however, they go down to less than 3.10^{-6}% and 0.001%, respectively. This is presumably due to small inaccuracies introduced by the piston movement which vanish when the piston stops moving (at $t \simeq 12$ s). The fairly low value of k_2, less than 13 times N_Γ in all the computations, shows the well-posedness of the problem boundary conditions, especially in the corner double nodes.

The results can be compared with data available in the literature. Our vertical run-up (4.25 m at $t = 27.8$ s) is in

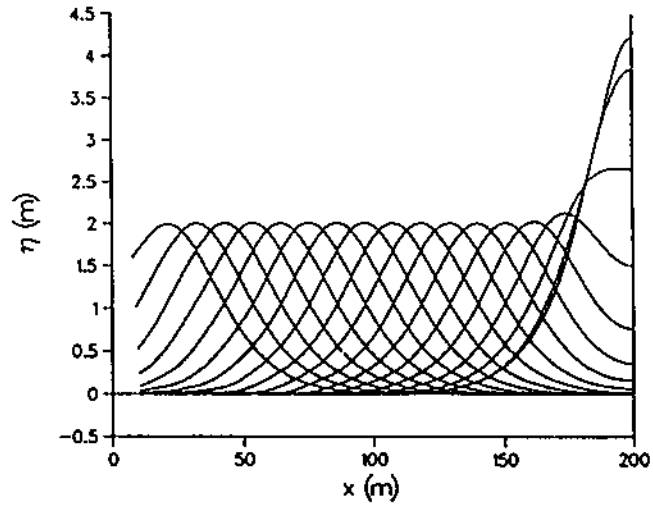

Fig. 8. Solitary wave (H/d = *0.2*, d = *10 m*, dt = *0.2 s*). *Run-up (90 deg.), 11 to 28 s, each 1 s*

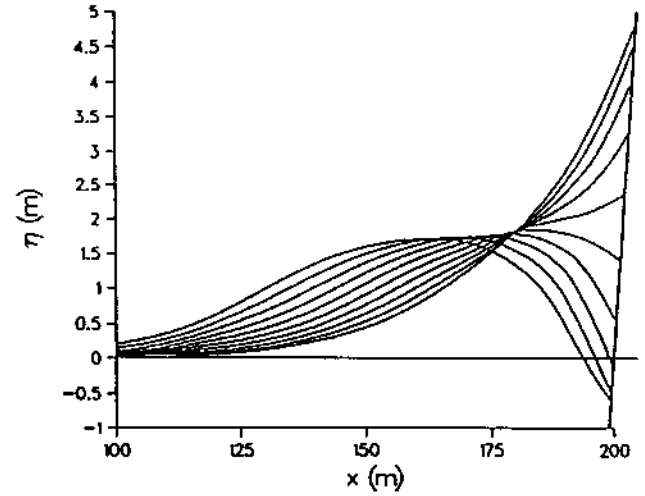

Fig. 9. Solitary wave (H/d = *0.2*, d = *10 m*, dt = *0.2 s*). *Run-down (45 deg.), 29 to 32.6 s, each 4 s*

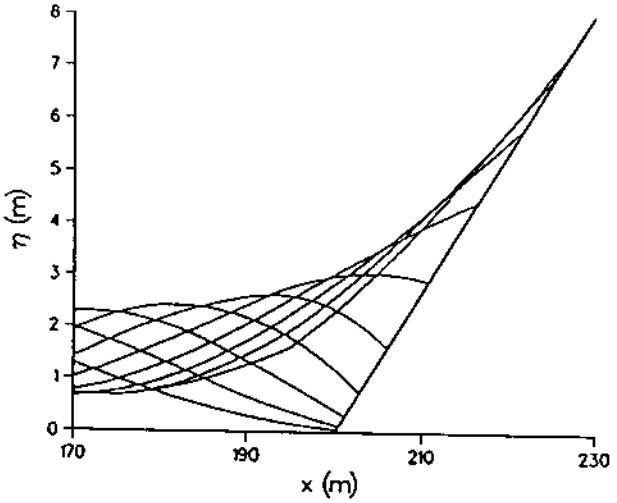

Fig. 10 Solitary wave (H/d = *0.2*, d = *10 m*, dt = *0.20 s*). *Run-up (15 deg.), 23 to 32 s, each 1 s*

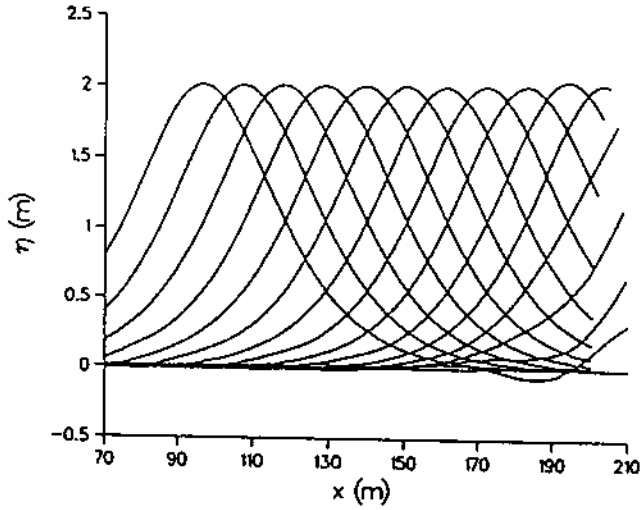

Fig. 11. Solitary wave (H/d = *0.2*, d = *10 m*, dt = *0.2 s*). *Radiation, 18 to 32 s, each 1 s*

complete agreement with Nakayama's[27] numerical results and with experimental results. Our 45 degree run-up (4.89 m at $t = 28.8$ s) is slightly less than the one computed by Kim *et al.*[17] (5.04 m), and the same applies to our run-up on a 15 degree slope (7.54 at $t = 32.6$ s instead of 7.66 m). In the Kim *et al.* study, however, the time development of the run-up is performed in a manner which, for small steepness of the slope may influence the accuracy of the solution substantially while in our model, we follow the particle motion exactly. Thus, we believe that our results may be more accurate.

Finally, a radiation problem has been studied by imposing on the right vertical boundary of the domain, the radiation condition (7), which should be satisfied exactly for a wave of constant shape (Fig. 11). The wave stays almost unperturbed and propagates out of the domain as it should without 'feeling' the boundary. The procedure works well, up to 32.0 s, when the wave is almost out of the domain, with a residual elevation of less than 15% of its amplitude. After that, the solution starts to oscillate, presumably due to difficulties with the moving vertical boundary. In this computation, a maximum of 8 iterations were used in the radiation boundary condition. However that only increased the C.P.U. time per step by 15%.

5.4. Transient wave generated by a wave maker

Generation of a periodic wave from a state of rest creates a transient problem, which has been studied by Lin, Newman and Yue[23], and Dommermuth and Yue[8].

Fig. 12 shows results for the case examined with $d = 50$ m, a computation region 700 m long and a wave period $T = 8.4$ s. The paddle wave maker was hinged at the bottom and oscillated sinusoidally in time with a maximum velocity of 2.0 m/s at the mean water surface. Thirty-three time steps were used per wave period for the wave which eventually became 7.1 m high and had a steepness of 6.5%. The boundary was discretized into 59 quadratic elements, with a total of 122 nodes, of which 71 were placed on the surface (approximately 13 per wave length).

The situation in Fig. 12 was obtained after 35 s which is almost as far as we have carried out the computation. It only shows the first 500 m of the computation region. Fig. 13 shows a blow-up of the first 200 m of the same wave motion.

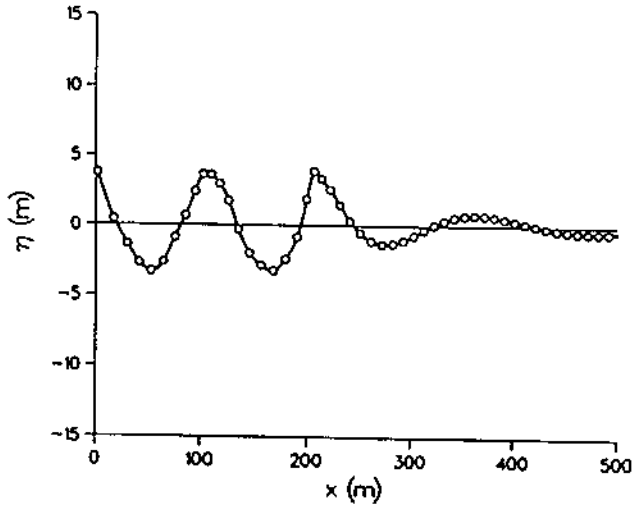

Fig. 12. Periodic wave (d = *50 m*, T = *8.4 s*, dt = T/*33 s*). *Time: 35.00 s*

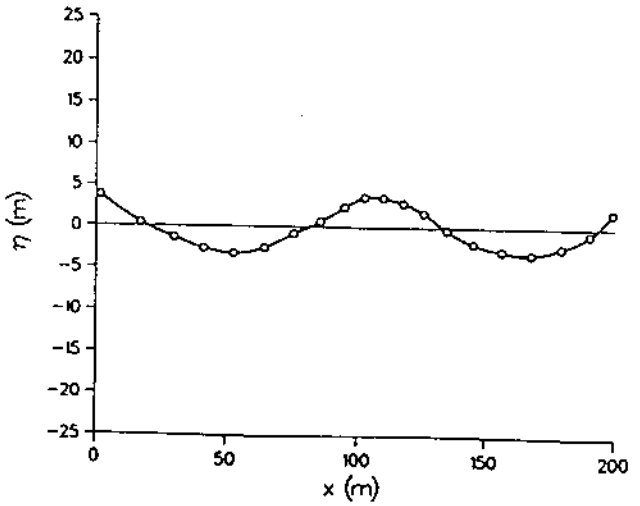

Fig. 13. Periodic wave (d = *50 m*, T = *8.4 s*, dt = T/*33 s*). *Time: 35.00 s*

From the computational results, however, it is evident that the radiation condition (7) does not work satisfactorily on the transient front of the waves.

6. CONCLUDING REMARKS

The computation examples presented here suggest that with sufficient accuracy in each of the steps, the Boundary Element Method may also be applied to more general wave problems than the development of space period waves for which is has proved to be so effective. Substantial amounts of development, however, are particularly needed for the absorption or radiation of the waves generated.

REFERENCES

1 Baker, G. R., Meiron, D. I. and Orszag, S. A. Generalized Vortex Method for Free-surface Flow Problems, *J. Fluid Mech.*, 1982, **123**, 477–501

2 Banerjee, G. R. and Butterfield, R. *Boundary Element Method in Engineering Science*, McGraw-Hill, UK., 1981

3 Brebbia, C. A. *The Boundary Element Method for Engineers*, John Wiley & Sons, UK, 1978

4 Brevig, P., Greenhow, M. and Vinje, T. Extreme Wave Forces on Submerged Wave Energy Devices, *Appl. Ocean Res.*, 1982, 4, 219–225

5 Brorsen, M. and Larsen, J. Source Generation of Nonlinear Gravity Waves with the Boundary Integral Method, *Coastal Engineering*, 1987, 11, 93–113

6 Bruch, E., Grilli, S. and Lejeune, A. Computation of the Fluid Flow in Zoned Anisotropic Porous Media and Determination of the Free Surface Seepage. In *Proc. 8th Intl. Conf. on Boundary Elements, Tokyo, Japan*, 1986 (ed. M. Tanaka and C. A. Brebbia), pp. 889–903, Springer-Verlag, Berlin

7 Dold, J. W. and Peregrine, D. H. Steep Unsteady Water Waves: An Efficient Computational Scheme. In *Proc. 19th Intl. Conf. on Coastal Engineering, Houston, USA*, 1984, p. 955–967

8 Dommermuth, D. G. and Yue, D. K. P. Numerical Simulation of Nonlinear Axisymmetric Flows with a Free Surface, *J. Fluid Mech.* 1987, 178, 195–219

9 Engquist, B. and Majda, A. Absorbing Boundary Conditions for the Numerical Simulation of Waves, *Math. of Computation*, 1977, 31, 629–651

10 Goring, D. G. Tsunamis – The Propagation of Long Waves onto a Shelf. *W. M. Keck Laboratory of Hydraulics and Water Resources, California Institute of Technology, Report No.* KH-R-38, 1978

11 Grilli, S. Etude de l'action de la houle sur les structures flottantes par éléments frontières. Comparaison avec les éléments finis. *Bull. de l'ATMA*, 1984, 84, 297–318

12 Grilli, S. The Numerical Modelling of the Wave Field near the Shore by the Boundary Element Method. In *Proc. Intl. Conf. on Environmental Software (ENVIROSOFT86), Los Angeles, USA*, 1986 (ed. P. Zannetti), pp. 471–486, Computational Mechanics Publication, Boston

13 Grilli, S. Application of the Boundary Element Method to some Elliptic Fluid Mechanics Problems. In *Proc. 1st Intl. Conf. on Computer Methods and Water Resources, Rabat, Morocco, 1988.* Vol. 4 (ed. D. Ouazar and C. A. Brebbia), pp. 97–113, Computational Mechanics Publications, Springer-Verlag, Berlin

14 Grilli, S. T., Skourup, J. and Svendsen, I. A. The Modelling of Highly Nonlinear Waves: A Step Toward the Numerical Wave Tank. Invited Paper in *Proc. 10th Intl. Conf. on Boundary Elements, Southampton, England*, 1988 (ed. C. A. Brebbia), Vol. 1, pp. 549–564, Computational Mechanics Publication, Springer-Verlag, Berlin

15 Hsiao, G. C. and McCamy, R. C. Solution of Boundary Value Problems by Integral Equations of the First Kind, *SIAM Rev.*, 1973, 15, 687–705

16 Isaacson, M. de St. Q. Nonlinear Effects on Fixed and Floating Bodies. *J. Fluid Mech.*, 1982, 120, 267–281

17 Kim, S. K., Liu, P. L.-F. and Liggett, J. A. Boundary Integral Equation Solutions for Solitary Wave Generation Propagation and Run-up, *Coastal Engineering*, 1983, 7, 299–317

18 Kravtchenko, J. Remarques sur le calcul des amplitudes de la houle linéaires engendrée par un batteur. In *Proc. 5th Intl. Conf. on Coastal Engineering*, 1954, pp. 50–61

19 Larsen, J. and Dancy, H. Open Boundaries in Short Wave Simulations – A New Approach, *Coastal Engineering*, 1983, 7, 285–297

20 Le Mehaute, B. Progressive Wave Absorber, *J. Hyd. Res.*, 1972, 10(2), 153–169

21 Liggett, J. A. and Liu, P. L.-F. Application of Boundary Element Methods in Fluid Mechanics. Chpt. 4 in *Topics in Boundary Element Research Vol. 1* (ed. C. A. Brebbia), Springer-Verlag, Berlin, 1984

22 Liggett, J. A. and Salmon, J. R. Cubic Spline Boundary Elements, *Intl. J. Numer. Meth. Engng*, 1981, 17, 543–556

23 Lin, W. M., Newman, J. N. and Yue, D. K. Nonlinear Forced Motion of Floating Bodies. In *Proc. 15th Intl. Symp. on Naval Hydrodynamics, Hamburg, Germany*, 1984

24 Liu, P. L.-F. and Liggett, J. A. Applications of Boundary Element Methods to Problems of Water Waves. Chpt. 3 in *Developments in Boundary Element Methods Vol. 2* (ed. P. K. Banerjee and R. P. Shaw), 1982, Applied Science Publishers Ltd, London

25 Liu, P. L.-F. and Liggett, J. A. Boundary Element Formulation and Solution for some Nonlinear Water Wave Problems. Chpt. 7 in *Developments in Boundary Element Methods Vol. 3* (ed. P. K. Banerjee), 1984, Applied Science Publishers Ltd, London

26 Longuet-Higgins, M. S. and Cokelet, E. D. The Deformation of Steep Surface Waves on Water – I. A Numerical Method of Computation, *Proc. R. Soc. Lond.*, 1976, A350, 1–26

27 Nakayama, T. Boundary Element Analysis of Nonlinear Water Wave Problems, *Intl. J. Numer. Meth. Engng*, 1983, 19, 953–970

28 Nam Seo, S. Time-Dependent Highly Nonlinear Waves (Ph.D. Dissertation), Civil Engineering Department, University of Delaware, USA, 1988

29 New, A. L., McIver, P. and Peregrine, D. H. Computation of Overturning Waves, *J. Fluid Mech.*, 1985, 150, 233–251

30 Rienecker, M. M. and Fenton, J. D. A Fourier Approximation Method for Steady Water Waves, *J. Fluid Mech.*, 1981, 104, 119–137

31 Shaw, R. P. Boundary Integral Equation Methods Applied to Wave Problems. Chpt. 6 in *Developments in Boundary Element Methods Vol 1*, 1979 (ed. P. K. Banerjee and R. Butterfield), Applied Science Publishers Ltd, London

32 Stroud, A. H. and Secrest, D. *Gaussian Quadrature Formulas*, Prentice-Hall International Inc., London, 1966

33 Svendsen, I. A. Mixed Boundary Value Problem for Laplace's Equation in Domain of Arbitrary Shape, *Technical University of Denmark Progress Report*, 1971, 23, 33–38

34 Vinje, T. and Brevig, P. Numerical Simulation of Breaking Waves, *Adv. Water Resources*, 1981, 4, 77–82

35 Yeung, R. W. Numerical Methods in Free Surface Flows, *Ann. Rev. Fluid Mech.*, 1982, 14, 395–442

36 Romate, J. E. The Numerical Simulation of Nonlinear Gravity Waves in Three Dimensions using a Higher Order Panel Method (Ph.D. Dissertation), Delft Hydraulics, The Netherlands, 1989.